Inspection 13.2 nm table-top full-field microscope

F. Brizuela,[1,*] Y. Wang,[1] C. A. Brewer,[1] F. Pedaci,[1] W. Chao,[2] E. H. Anderson,[2] Y. Liu,[2] K. A. Goldberg,[2] P. Naulleau,[2] P. Wachulak,[1] M. C. Marconi,[1] D. T. Attwood,[2] J. J. Rocca,[1] and C. S. Menoni[1]

NSF ERC for Extreme Ultraviolet Science and Technology
[1]Colorado State University, Fort Collins, CO 80523, USA
[2]Center for X-ray Optics, Lawrence Berkeley National Laboratory, Berkeley, CA 94720, USA
[*]Corresponding author: brizuela@engr.colostate.edu

ABSTRACT

We present results on a table-top microscope that uses an EUV stepper geometry to capture full-field images with a half-pitch spatial resolution of 55 nm. This microscope uses a 13.2 nm wavelength table-top laser for illumination and acquires images of reflective masks with exposures of 20 seconds. These experiments open the path to the realization of high resolution table-top imaging systems for actinic defect characterization.

Keywords: extreme ultraviolet lithography, EUV, mask inspection, actinic inspection, EUV laser.

1. FULL-FIELD, LASER-BASED, ACTINIC MICROSCOPE SETUP

Advances in extreme ultraviolet lithography (EUVL) drive the development of inspection tools capable of detecting and characterizing printable defects on EUVL masks. The need for actinic or at-wavelength inspection of printable defects buried in the Mo/Si multilayer coatings, that would otherwise go undetected using visible/ultraviolet light, is well recognized [1]. Full-field actinic microscopes produce a magnified aerial image of the mask and allow the evaluation of pattern and defect printability independently of the response of the photoresist. Furthermore, these microscopes can be useful for defect repair evaluation of EUVL masks [2]. Current synchrotron-based actinic microscopes have imaged amplitude and phase defects on EUVL masks with a spatial resolution better than 100 nm [3, 4]. In particular, the SEMATECH Berkeley tool, design to mimic the imaging conditions of EUVL steppers can obtain high quality images with 88 nm spatial resolution and acquisition times of 20 to 40 seconds [4]. This full-field microscope is routinely used to study EUVL masks.

The use of synchrotron light as the illumination source of full-field actinic microscopes limits the availability and accessibility of these tools. To expand the use of these microscopes, compact EUV sources capable of providing sufficient flux at ~13.5 nm are required. Table-top EUV lasers have been successfully used as illumination sources for the demonstration of compact full-field microscopes that have reached 38 nm spatial resolution [5-8]. Their high brightness and moderate coherence make them well suited for zone plate-based microscopy. Using this approach, we have developed a table-top full-field reflection microscope for EUVL mask defect characterization that can obtain images in 20 seconds with a spatial resolution of 55 nm, comparable to that obtained with synchrotron sources.

The microscope uses as illumination a nickel-like cadmium laser developed at Colorado State University. This laser operates at a wavelength of 13.2 nm with an average power of $\sim 1\times10^{14}$ W cm^{-2}, providing sufficient flux for reflection mode imaging [9, 10]. Its narrow bandwidth ($\Delta\lambda/\lambda < 1\text{x}10^{-4}$) makes it ideal for zone plate based microscopy, decreasing chromatic aberrations introduced by the objective. The laser pulses are created at a repetition rate of 5 Hz by heating a 4 mm wide Cd target using a sequence of pulses from a chirped-pulse-amplification Ti:Sapphire laser system. In this scheme, a 120 ps pre-pulse is line-focused onto the target generating a Cd plasma that is allowed to expand to reduce density gradients. After a selected time delay a second 6.7 ps pulse impinges on the plasma at a 23^{o} grazing incidence angle. This pulse heats the plasma to create a transient population inversion in the $4d^1S_0$-$4p^1P_1$ transition, allowing the amplification of spontaneous emission of 13.2 nm wavelength light.

Alternative Lithographic Technologies, edited by Frank M. Schellenberg, Bruno M. La Fontaine
Proc. of SPIE Vol. 7271, 72713F · © 2009 SPIE · CCC code: 0277-786X/09/$18 · doi: 10.1117/12.814320

The 13.2 nm reflection microscope was designed to mimic the illumination conditions of a 0.25 NA, 4× demagnification EUVL stepper as described by A. Barty et al. [11]. This configuration, first employed at the SEMATECH Berkeley actinic microscope allows a more in-depth understanding of the printability of patterns and defects onto the silicon wafers [4]. To meet this criteria with the microscope, the angle of illumination is set to 6 degrees from normal, the objective zone plate numerical aperture (NA) is selected equal to 0.0625 NA to match a 0.25 NA of a 4× demagnification EUVL stepper, and the imaging process is maintained incoherent by matching condenser's NA to the objective's NA and employing the 13.2 nm laser which has moderate coherence (coherence length 1/20 beam diameter).

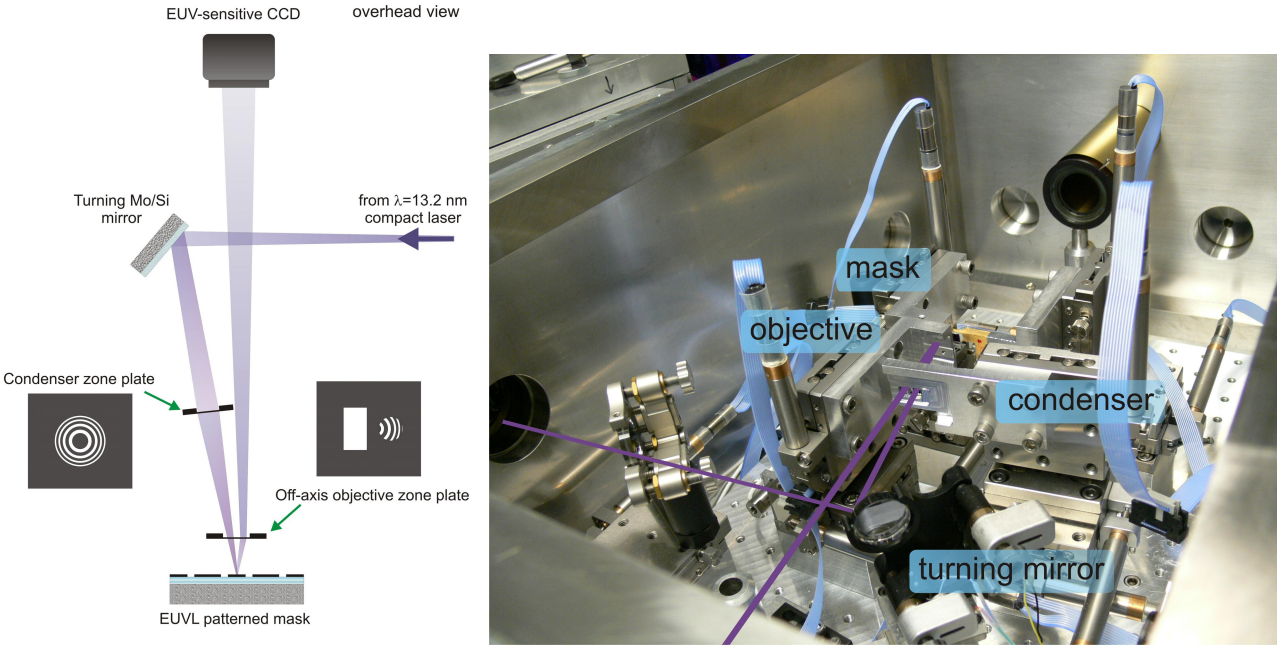

Fig. 1. Schematic illustration of the geometry (not to scale) and picture of the laser-based EUV microscope. The optics were designed to mimic the imaging conditions of a 4×, 0.25 NA EUVL stepper.

The setup of the microscope and an image of the instrument are shown in Figure 1. In this setup the laser is guided by a flat Mo/Si mirror to a condenser zone plate that collects the laser beam and illuminates the mask at an incident angle of 6°. The 5 mm diameter condenser, produced by e-beam lithography onto a 100 nm thick Si_3N_4 membrane, is located at ~35 cm from the output of the laser to match the beam diameter [12]. Its focal length and numerical aperture at 13.2 nm wavelength are 38 mm and 0.066 respectively. The light reflected off the sample is collected by an objective zone plate. The objective zone plate is an off-axis sub-aperture of a full parent zone plate lens that would have a 330 µm diameter, an outer zone width of 40 nm, and a focal length of 1 mm. The pupil diameter is 120 µm, defining a NA of 0.0625, and its center is displaced 100 µm from the axis of the parent zone plate. An uncoated rectangular aperture next to the off-axis objective zone plate transmits the incoming condensed laser beam illumination. A scanning electron micrograph is shown in Figure 2 where the outline of the parent zone plate is marked with a dashed line. To increase the transmission through this aperture, the Si_3N_4 membrane was thinned to 40 nm. The off-axis zone plate enables near-normal incidence imaging of the mask surface, minimizes aberrations, and provides incoherent illumination conditions by matching the NA of the condenser [13]. The off-axis zone plate projects the image directly onto an EUV-sensitive CCD detector located parallel to the EUVL mask. The entire microscope is housed in a in a 70×45×40 cm^3 vacuum chamber.

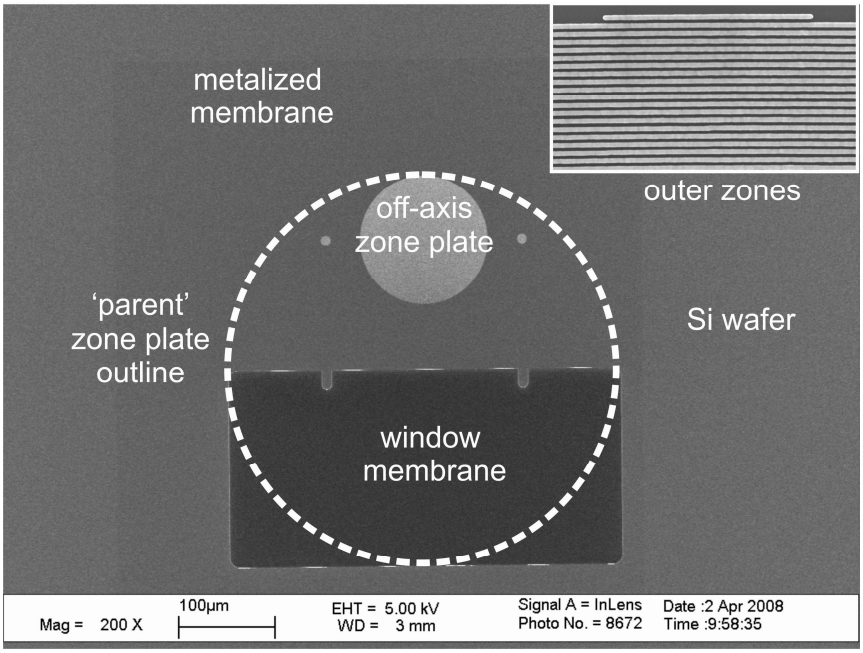

Figure 2. b) SEM images of the off-axis zone plate and uncoated window region were the dashed line indicates the extent of the 'parent' zone plate. The insert shows the 40 nm half-pitch outer zones of the objective zone plate.

2. IMAGE ACQUISITION AND MICROSCOPE EVALUATION

The imaging capabilities of the microscope were evaluated using a sample consisting of a Mo/Si multilayer coated Si wafer onto which bright-field Ni absorber grating patterns with half-pitch sizes ranging from 80 nm to 500 nm were patterned. The bright-field sample allows for the simultaneous evaluation of the resolution of the microscope as well as the quality of the illumination employed.

Figure 3 shows several actinic images of elbow patterns with half-pitch values of 80 nm, 100 nm, 120 nm and 140 nm. The images were obtained with exposure times of 20 seconds, comparable with exposure times used at synchrotron based microscopes. The images have a field of view of approximately 5×5 μm^2 with a pixel size corresponding to ~22 nm in the sample plane. The images were taken with static illumination which gives rise to some inhomogeneities in intensity. Nevertheless, as shown in the intensity cross sections shown below each image, even for the smallest grating, 80 nm half-period, the modulation exceeds 60% indicating that the features are well above the resolution threshold of the microscope.

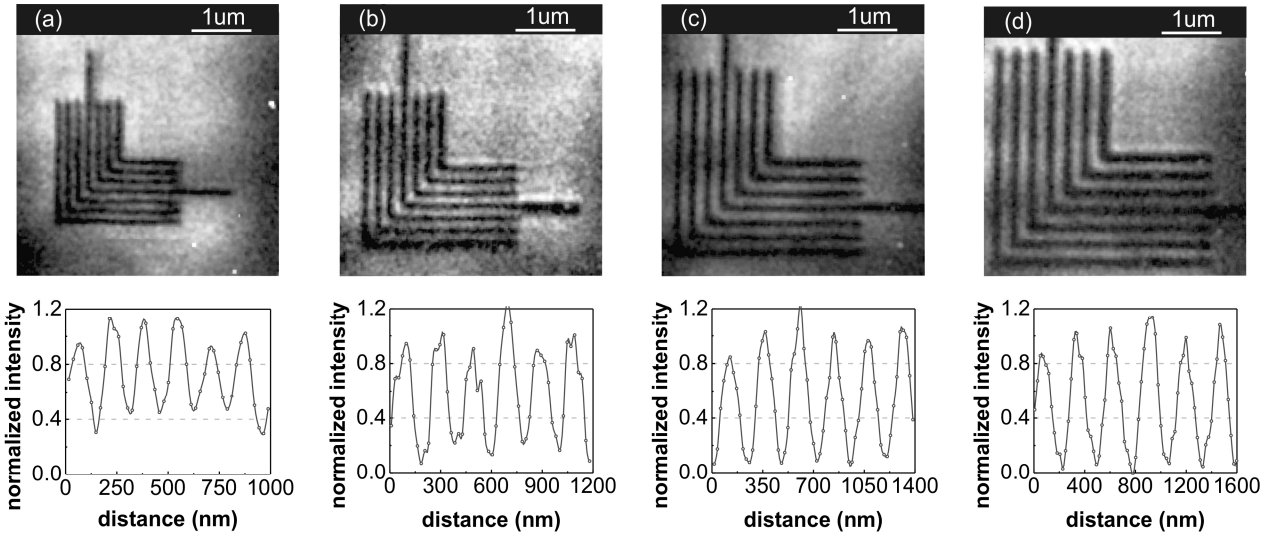

Figure 3. Fully resolved actinic images and intensity lineouts of elbow patterns with: a) 80 nm, b) 100 nm, c) 120 nm, and d) 140 nm half-pitch. The images were obtained with 20 second exposures and ~610× magnification. The intensity lineouts were obtained by averaging five rows of pixels (~100 nm on the mask) across the gratings.

In the absence of smaller gratings, the spatial resolution limit of the microscope was evaluated using knife-edge measurements across large (>2 μm) absorber patterns as shown in Figure 4. For an incoherent imaging system such as this microscope, the 10% to 90 % intensity transition across a sharp edge of a feature corresponds to twice the half-pitch resolution value that would be obtained applying the Rayleigh resolution criterion for gratings [13]. From Figure 4, a 10% to 90% transition value of 110±5 nm, was obtained, corresponding to a half-pitch spatial resolution value of 55±3 nm.

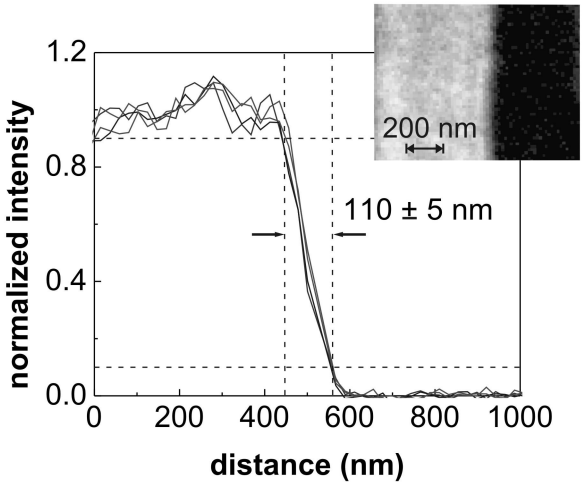

Figure 4. Knife-edge test for the EUV image shown in the insert. The 10% to 90% transition is 110±5 nm.

The spatial resolution limit was independently confirmed by analyzing the EUV images of Figure 3 with a full-image correlation method described by Wachulak and collaborators [14]. With this method, the image spatial resolution is obtained by comparing an EUV image with a series of templates of varying spatial resolution. To create these templates, a portion of the original image is used. Low spatial frequency components associated with slowly varying illumination are filtered out in the spectral domain. After further filtering to remove "salt and pepper" noise, a skeletonizing algorithm is applied to create a matrix containing the location of the features on the image. The features represented by this matrix are one pixel wide and resemble the patterns of the original image in shape and position. This matrix is convolved with a circle of radius r_c to generate a template of features with widths of $2r_c$ and a spatial resolution given by the pixel element size of the original image file. From this template, a subset of lower spatial resolution templates is generated. This is done by reducing the first template by an integer factor ranging from 1 to 15 and extrapolated back to the original size. This operation produces a loss of high frequencies in the new templates, resulting in a decrease in spatial resolution. The process is then repeated for different values of r_c. This generates a matrix of templates with two variables: the width of the features being imaged, $2r_c$, and the resolution of the imaged features. In the final step, all the templates of this matrix are correlated with the original EUV image generating a correlation map from which the image resolution and object's critical dimension are obtained. Figure 5 shows a plot of the correlation coefficient versus half-pitch spatial resolution obtained when the image analysis method was applied to the 120 nm half-pitch elbow image on the left. This method was applied to several images resulting in a spatial resolution of 53±10 nm. This value is in agreement with the knife-edge measurements and with the expected resolution for the imaging system.

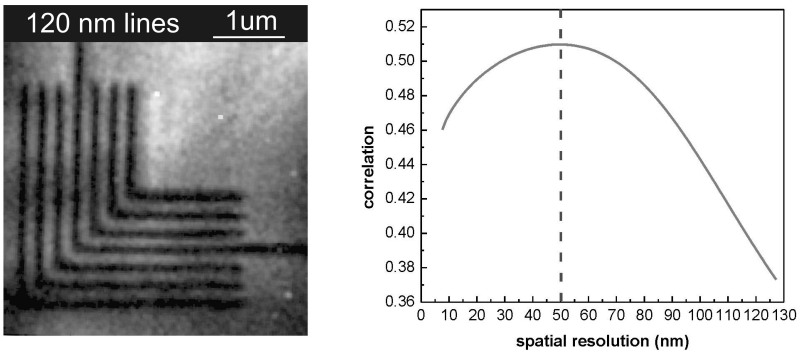

Figure 5. Full-image correlation method to determine the resolution of the microscope applied to an image of a 120 nm half-period elbow pattern. The correlation values between a template of 120 nm half-period (r_c=80) at different resolution values and the original image are shown in the plot.

The modulation transfer function (MTF) of the microscope (Figure 6) was obtained combining the intensity cross section measurements of Figure 3 with the resolution measurements of Figures 4 and 5. The resulting transfer function is in agreement with the expected MTF for a 0.0625 NA objective illuminated with 13.2 nm light. Considering a 4× demagnification system, the spatial resolution of this microscope, 55 nm, would correspond to a printed feature size on the wafer of ~14 nm, meeting the specifications set for the 22 nm technology half-pitch node.

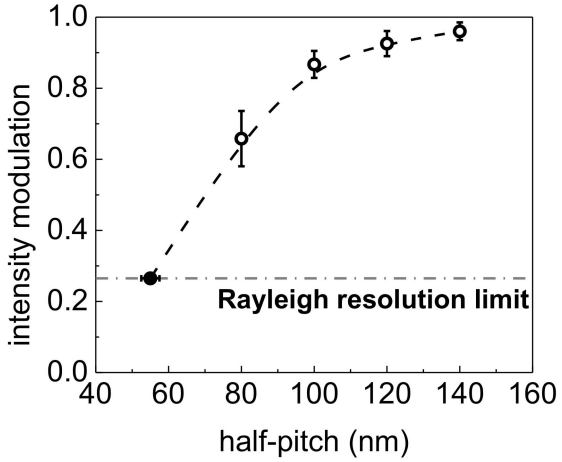

Figure 6. Microscope's modulation transfer function constructed using the lineouts from the images of Fig. 2 (open circles) and the knife-edge test (solid circle).

3. SUMMARY

In summary, we have demonstrated an actinic table-top EUV reflection microscope that, emulating the incoherent illumination conditions of a EUVL stepper, can obtain images of absorber patterns in Mo/Si EUVL masks with a spatial resolution of 55 nm in 20 second exposures. These parameters are comparable with current synchrotron based full-field actinic microscopes. It is forecasted that improvements in the throughput of the imaging system and of the illumination source will reduce exposure times to a few seconds. The demonstration of a table-top EUV actinic microscope for EUVL lithography opens the path for the development of on-site test beds that could further advance the development of this lithographic technique into a viable commercial option.

We acknowledge the contribution of Dr. Georgiy Vaschenko and the support of the Engineering Research Centers Program of the National Science Foundation under NSF Award Number EEC-0310717.

REFERENCES

1. K. A. Goldberg, A. Barty, Y. Liu, P. A. Kearney, Y. Tezuka, T. Terasawa, J. S. Taylor, H.-S. Han, and O. R. I. Wood, "Actinic inspection of extreme ultraviolet programmed multilayer defects and cross-comparison measurements," Journal of Vacuum Science and Technology B **24**, 2824-2828 (2006).
2. K. A. Goldberg, A. Barty, P. Seidel, K. Edinger, R. Fettig, P. A. Kearney, H.-S. Han, and O. R. I. Wood, "EUV and non-EUV inspection of reticle defect repair sites," in *Emerging Lithographic Technologies XI, SPIE Advanced Lighography*, (Proc. SPIE, 2007), 6517-6511.
3. M. Osugi, K. Takana, N. Sakaya, K. Hamamoto, T. Watanabe, and H. Kinoshita, "Resolution Enhancement of Extreme Ultraviolet Microscope Using an Extreme Ultraviolet Beam Splitter," Japanese Journal of Applied Physics **47**, 4872-4977 (2008).

4. K. A. Goldberg, P. P. Naulleau, I. Mochi, E. H. Anderson, S. B. Rekawa, C. D. Kemp, R. F. Gunion, H.-S. Han, and S. Huh, "Actinic extreme ultraviolet mask inspection beyond 0.25 numerical aperture," Journal of Vacuum Science and Technology B **26**, 2220-2224 (2008).
5. C. A. Brewer, F. Brizuela, P. Wachulak, D. H. Martz, W. Chao, E. H. Anderson, D. T. Attwood, A. V. Vinogradov, I. A. Artyukov, A. G. Ponomareko, V. V. Kondratenko, M. C. Marconi, J. J. Rocca, and C. S. Menoni, "Single-shot extreme ultraviolet laser imaging of nanostructures with wavelength resolution," Optics Letters **33**, 518-520 (2008).
6. F. Brizuela, G. Vaschenko, C. Brewer, M. Grisham, C. S. Menoni, M. C. Marconi, J. J. Rocca, W. Chao, J. A. Liddle, E. H. Anderson, D. T. Attwood, A. V. Vinogradov, I. A. Artioukov, Y. P. Pershyn, and V. V. Kondratenko, "Reflection mode imaging with nanoscale resolution using a compact extreme ultraviolet laser," Optics Express **13**, 3983-3988 (2005).
7. G. Vaschenko, C. Brewer, E. Brizuela, Y. Wang, M. A. Larotonda, B. M. Luther, M. C. Marconi, J. J. Rocca, and C. S. Menoni, "Sub-38 nm resolution tabletop microscopy with 13 nm wavelength laser light," Optics Letters **31**, 1214-1216 (2006).
8. G. Vaschenko, F. Brizuela, C. Brewer, M. Grisham, H. Mancini, C. S. Menoni, M. C. Marconi, J. J. Rocca, W. Chao, J. A. Liddle, E. H. Anderson, D. T. Attwood, A. V. Vinogradov, I. A. Artioukov, Y. P. Pershyn, and V. V. Kondratenko, "Nanoimaging with a compact extreme-ultraviolet laser," Optics Letters **30**, 2095-2097 (2005).
9. J. J. Rocca, Y. Wang, M. A. Larotonda, B. M. Luther, M. Berrill, and D. Alessi, "Saturated 13.2 nm high-repetition-rate laser in nickellike cadmium," Optics Letters **30**, 2581-2583 (2005).
10. Y. Wang, M. A. Larotonda, B. M. Luther, D. Alessi, M. Berrill, V. N. Shyaptsev, and J. J. Rocca, "Demonstration of high-repetition-rate tabletop soft-x-ray lasers with saturated output at wavelengths down to 13.9 nm and gain down to 10.9 nm," Physical Review A **72**(2005).
11. A. Barty, J. S. Taylor, R. Hudima, E. Spiller, D. W. Sweeney, G. Shelden, and J.-P. Urbach, "Aerial Image Microscopes for the inspection of defects in EUV masks," in *22nd Annual BACUS Symposium on Photomask Techology*, (proceedings of SPIE, 2002), 0277-0786X/0202.
12. E. H. Anderson, "Specialized Electron Beam Nanolithography for EUV and X-Ray Diffractive Optics," IEEE Journal of Quantum Electronics **42**, 27-35 (2006).
13. J. M. Heck, D. T. Attwood, W. Meyer-Ilse, and E. Anderson, "Resolution determination in X-ray microscopy: an analysis of the effects of partial coherence and illumination spectrum," Journal of X-Ray Science and Technology **8**, 95-104 (1998).
14. P. W. Wachulak, C. A. Brewer, F. Brizuela, C. S. Menoni, W. Chao, E. H. Anderson, R. A. Bartels, J. J. Rocca, and M. C. Marconi, "Analysis of extreme ultraviolet microscopy images of patterned nanostructures based on a correlation method," Journal of the Optical Society of America B **25**, B20-B26 (2008).